Received: 16 October 2024 | Revised: 12 December 2024 | Accepted: 28 December 2024

Electrical Materials and Applications

DOI: 10.1049/ema3.70011

ORIGINAL RESEARCH

$BaZrO_3$-modified (K, Na)NbO_3-based lead-free piezoceramics: High unipolar fatigue resistance

Jun Ma[1,2] | Tao Lin[1,2] | Chuanyang Tao[1,2] | Yuqing Zhou[1,2] | Meipeng Zhong[1] | Yi-Xuan Liu[3,4] | Zhongshang Dou[5] | Binjie Chen[5] | Shulin Tan[6] | Xin Ma[7] | Qiang He[8] | Wen Gong[9] | Fang-Zhou Yao[5,10] | Ke Wang[4,5]

[1]College of Mechanical and Electrical Engineering, Jiaxing Nanhu Unversity, Jiaxing, China

[2]College of Mechanical and Electrical Engineering, Wenzhou University, Wenzhou, China

[3]Department of Materials Science and Metallurgy, University of Cambridge, Cambridge, UK

[4]State Key Laboratory of New Ceramics and Fine Processing, School of Materials Science and Engineering, Tsinghua University, Beijing, China

[5]Research Center for Advanced Functional Ceramics, Wuzhen Laboratory, Jiaxing, China

[6]Physical Chemistry Department, Technical University of Darmstadt, Darmstadt, Germany

[7]Shanghai Sixth People's Hospital Affiliated to Shanghai Jiao Tong University School of Medicine, Shanghai, China

[8]China Electric Power Research Institute, Beijing, China

[9]Tongxiang Tsingfeng Technology Co. Ltd., Jiaxing, Zhejiang, China

[10]Center of Advanced Ceramic Materials and Devices, Yangtze Delta Region Institute of Tsinghua University, Jiaxing, Zhejiang, China

Correspondence

Meipeng Zhong, Yi-Xuan Liu, Shulin Tan and Xin Ma.

Email: zhongmeipeng@jxnhu.edu.cn, liuyx2022@mail.tsinghua.edu.cn, tanshulin@gmail.com and maxin@sjtu.edu.cn

Funding information

the Program for Jiaxing Leading Innovative and Entrepreneurial Teams; National Natural Science Foundation of China, Grant/Award Numbers: 52032005, 52325204, U22A20254; Key Research and Development Program of Zhejiang Province, Grant/Award Number: 2022C01229

Abstract

(K, Na)NbO_3-based lead-free piezoelectric materials are considered a promising candidate to replace a lead-containing counterpart in actuator applications, with electrical fatigue being a major concern during this transition. This study elaborates on a promising material with a nominal composition of $0.92(K_{0.5}Na_{0.5})NbO_3$-$0.02(Bi_{0.8}Li_{0.2})TiO_3$-$0.06BaZrO_3$ (BZ6) and evaluates its unipolar fatigue resistance. After 10^7 cycles of unipolar fatigue, the strain variation of the BZ6 ceramic is within 8% of its initial value, and both its $S(E)$ and $\varepsilon_{33}(E)$ curves exhibit less pronounced asymmetry than that of PIC151. Strain asymmetry and the development of internal bias fields are observed in the composition, which originates from the agglomeration of space charge during unipolar cycling. The post-annealing treatment allows the full restoration of electrical properties for the fatigued BZ6 ceramic, making it highly suitable for actuator applications.

KEYWORDS

(K, Na)NbO_3, electrical properties, lead-free piezoceramics, unipolar fatigue resistance

1 | INTRODUCTION

Piezoelectric ceramics are functional materials that can convert mechanical energy into electrical energy and vice versa.[1–5] They have been proven to have diverse applications in electronic and power devices, such as actuators, ultrasonic transducers, energy harvesters, smart sensors etc. For example, piezoelectric sensors are used for real-time monitoring of electrical equipment, helping maintenance personnel to detect equipment failures promptly, thereby ensuring the safety and reliability of the power system. And piezoelectric materials are also applied in ultrasonic detection technology to effectively identify defects and failures

within electrical equipment.[6,7] Through these innovative applications, piezoelectric materials not only enhance the operational efficiency of the state grid but also promote the intelligence and sustainable development of the power system. The lead-containing piezoelectrics represented by $Pb(Zr,Ti)O_3$ (PZT) dominates the market due to the exceptional comprehensive performance. However, PZT-based ceramics are confronted with increasing concerns over the adverse environmental and human health issues of toxic lead. As government regulations on lead content in ceramic components become stricter, these concerns are heightened, driving the piezoelectric materials research community to shift focus towards the development of new environmentally benign alternatives.

Potential candidate materials considered to replace lead-containing compounds in applications include potassium sodium niobate (KNN),[8,9] bismuth sodium titanate (NBT),[10] and barium titanate (BT).[11,12] Recently, Zhang et al. selected the $(0.98-x)(K_{0.5}Na_{0.5})NbO_3-0.02(Bi_{0.5}Li_{0.5})TiO_3-xBaZrO_3$ system as a prototype for the engineering-phase composition of KNN-based piezoelectric ceramics. This system has demonstrated high electromechanical performance (normalised strain d_{33}* of 470 pm/V[13]), along with high relative density, low leakage current, and fracture toughness. Enhanced domain wall contributions and improved domain wall mobility are considered reasons for the high electromechanical performance of the investigated lead-free KNN system. However, practical applications not only require excellent piezoelectric performance but also reliability and long-term stability during cyclic electrical loading to ensure a successful industrial implementation.

For actuator applications of piezoelectric components, the most common electrical loading scenario is the unipolar drive mode, where the electrical signal cycles between zero and maximum field without reversing polarity.[14–16] However, unipolar cycling often induces fatigue effects, as demonstrated by deteriorated unipolar strain and polarisation and emergence of internal bias (E_{bias}), which can affect component performance and service life.[17–19] For PZT family materials, although there are a large number of fatigue research literature available for references,[20,21] the charge agglomeration model is frequently cited to explain the unipolar fatigue behaviour of PZT ceramics, which reveals the redistribution of charge carriers and their agglomeration at grain boundaries and internal defects during the cycle.[22–24] However, it is worth mentioning that the fatigue research of KNN-based ceramic materials is still relatively scarce.[25–28] In addition, for newly developed lead-free ceramics, such as BZ6-based materials, the traditional PZT fatigue model may not be fully applicable.[29–31] Therefore, it is particularly urgent and important to study the fatigue characteristics of these promising lead-free compositions in depth. In order to further improve the unipolar fatigue resistance of lead-free materials, it is highly demanded to understand the mechanism of unipolar fatigue.

This study investigated the unipolar fatigue behaviour of $0.92(K_{0.5}Na_{0.5})NbO_3-0.02(Bi_{0.5}Li_{0.5})TiO_3-0.06BaZrO_3$ (BZ6) piezoelectric ceramics. The results indicate that BZ6 ceramics exhibit excellent unipolar fatigue resistance comparable to commercially available soft PZT. After 10^7 cycles, BZ6 ceramics showed no significant degradation in unipolar strain, coupled with good piezoelectric performance, making this system a promising candidate for actuator applications. Due to the striking similarity in unipolar fatigue characteristics between BZ6 and PIC151 ceramics, the agglomeration of space charges could also be applicable to rationalise the mild unipolar fatigue behaviour of BZ6 ceramics.

2 | EXPERIMENTAL PROCEDURE

2.1 | Sample preparation procedure

The ceramic samples with a composition of $0.92(K_{0.5}Na_{0.5})NbO_3-0.02(Bi_{0.8}Li_{0.2})TiO_3-0.06BaZrO_3$, henceforth denoted as BZ6, were meticulously crafted through the conventional solid-phase reaction technique. Employing a selection of high-purity raw materials—Na_2CO_3, K_2CO_3, Nb_2O_5, Bi_2O_3, Li_2CO_3, TiO_2, $BaCO_3$, and ZrO_2, the process began with a 24-h drying phase at 120°C. These constituents were then accurately weighed to adhere to stoichiometric ratios. Following this, the ingredients were immersed in ethanol and mixed for 24 h at a consistent 300 r/min, utilising zirconia balls to achieve a uniform dispersion. Post-mixing, the mixture was subjected to a second drying phase at 120°C. The resultant powder was first calcined in a sealed alumina crucible at 730°C for a duration of 4 h, marking the initial stage of heat treatment. Subsequently, the powder was processed through a 24-h ball-milling regimen at 300 r/min, followed by a third drying phase at 120°C. The powder was then meticulously sieved through a 60-mesh screen. As the process advanced, the powder underwent a second calcination at 930°C for 4 h. In preparation for this, 1.0 wt.% MnO_2 (procured from China National Pharmaceutical Group Corporation) was introduced as a sintering aid, maintaining the established milling parameters. The sintered powder was then transformed into discs, each 10 mm in diameter and 1.5 mm thick, under a uniaxial pressure of 10 MPa. These discs were further subjected to cold-isostatic pressing at 200 MPa, employing filler powder of the same composition (LDJ-100/320-300, Chuan-Xi, China). The final step involved sintering the discs at 1150°C for a period of 5 h, culminating in the formation of the BZ6 ceramic samples.

The thickness of as-sintered samples was reduced to 1 mm, and then the two surfaces of the samples were polished to a mirror-like surface by using a diamond polish with a grain size of 3 μm, 1 μm, and 0.04 μm successively. It was shown that the quality of electrode-surface contact had a significant effect on the fatigue properties. In order to characterise the electrical properties and electrodeposition, silver electrodes were coated on both sides of the samples and sintered at 600°C for 30 min. The samples were polarised in silicon oil at 120°C for 30 min

under an electric field of 3 kV/mm for the measurement of piezoelectric constant d_{33}.

2.2 | Sample characterisations

The surface microstructure of the polished samples was studied by means of a scanning electron microscope (SEM, Sigma 300, ZEISS, Germany) equipped with an energy dispersive X-ray (EDX) detector. For the piezoresponse force microscope (PFM) observation, the samples after sintering were polished to about 1000 μm in thickness. The PFM experiments were performed using a commercial PFM (PFM, Jupiter XR, OXFORD INSTRUMENTS, UK). The DC voltage signal was applied for the local ferroelectric and piezoelectric measurements. The domain morphologies were also observed using a high-resolution transmission electron microscopy (TEM, F 200, Japan) operated at 200 kV.

The crystal structure of the samples was measured by an X-ray diffractometer (XRD, D8 ADVANCE, BRUKER, Germany) using Cu Kα1 radiation with a scanning speed of 0.05°/s in the 2θ range from 20° to 60°. A quasi-static piezoelectric d_{33} metre (ZJ-3A, Institute of Acoustics, Chinese Academy of Sciences, Beijing, China) was used to measure the piezoelectric constant d_{33} of the polarised samples after ageing for about one day at room temperature. The electrical properties of the samples were tested using a ferroelectric measurement system (TF Analyser 2000E, aixACCT Systems GmbH, Aachen, Germany). This includes the large-signal hysteresis return $P(E)$ and strain-electric field $S(E)$ curves and the small-signal piezoelectric constant-electric field $d_{33}(E)$ curve and dielectric constant-electric field $\varepsilon_{33}(E)$ curve. The electrical properties of the fatigued samples were tested again after annealing at 300°C for half an hour to investigate the effect of annealing on their fatigue properties. To ensure the consistency and reproducibility of the experiments, at least three samples were tested.

Fatigue tests were performed using a unipolar triangular electrical signal with an amplitude of 2 kV/mm ($2E_C$) at a frequency of 50 Hz for a total of 1×10^7 cycles. Subsequently, the ceramics were measured using a TF Analyser 2000E ferroelectric measurement system at a frequency of 10 Hz and 3 kV/mm.

3 | RESULTS AND DISCUSSION

3.1 | Unipolar fatigue properties of $BaZrO_3$-doped (K, Na)NbO_3 ceramics

Figure 1 presents the X-ray diffraction (XRD) pattern of the BZ6 ceramics, which reveals the characteristic features of a typical perovskite structure. A critical analysis of the relative intensity ratio, I_{002}/I_{200}, near the $2\theta = 45°$, is conventionally employed to discern the phase structure of (K, Na)NbO_3-based ceramics. For piezoelectric ceramics with a tetragonal symmetry that are randomly oriented, the I002/I200 ratio is 1:2. A single rhombohedral (R) phase shows only one (200) peak. The crystallographic diffraction spectrum, magnified to highlight the <002> planes, as depicted in Figure 1b, clearly demonstrates the coexistence of both rhombohedral and tetragonal phases within the BZ6 ceramics. Extensive research studies have underscored that compositions rich in the tetragonal phase are endowed with enhanced fatigue resistance. Complementing the XRD analysis, the scanning electron microscopy (SEM) image of the BZ6 ceramics' surface, as shown in Figure 1c, unveils an intricate mosaic of irregular polygonal grains interspersed with notable porosity. To further quantify the microstructural attributes, the grain size distribution of the BZ6 ceramics was analysed using a nano measurer software. The average grain size (Ga) obtained by analysis is 2.28 mm, and it can be seen from the figure that the material uniformity of BZ6-based ceramics is good, and the uneven grain size may lead to local stress concentration and affect the fatigue strength of the material. It provides a quantitative description of the material's microstructure and provides insights into its potential mechanical and electrical properties.

Piezoresponse force microscopy (PFM) has established itself as an essential tool in the analytical arsenal, providing unparaleled insights into the origins of the unique piezoelectric properties that materials exhibit at the nanoscale. In this study, we harnessed the power of PFM to examine the domain morphology of the BZ6 ceramic, as illustrated in Figure 2a. The amplitude image, captured through out-of-plane PFM (VPFM), unveils a complex array of strip-like nano domains. It is posited that the presence of these domains plays a pivotal role in enhancing the piezoelectric response. Figure 2b showcases the domain morphology image

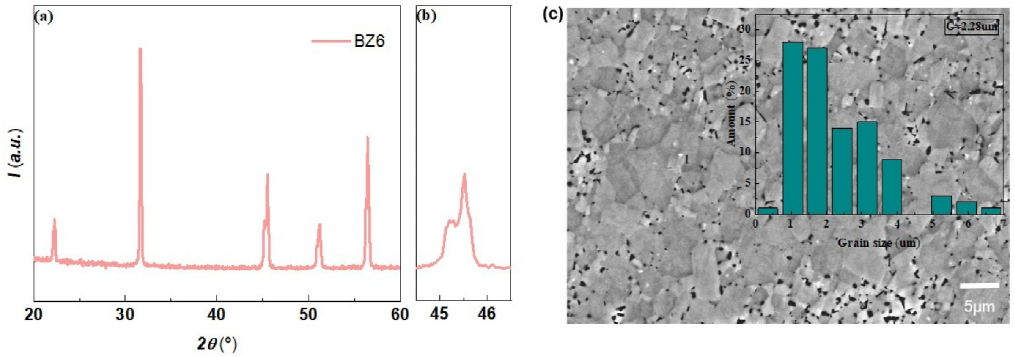

FIGURE 1 (a) The XRD pattern of BZ6 ceramics and (b) the enlarged (002) diffraction peak, as well as (c) the SEM morphology and grain size.

for BZ6. For the BZ6 sample, a 20-V voltage was found to be adequate for achieving full domain switching. This is evident in the phase contrast of the squares within the image, which stands out from the surrounding regions.

The strain curves of the BZ6 piezoelectric ceramics, both pre-fatigue and post-fatigue across varying cycles under unipolar electric fields, are elegantly portrayed in Figure 3a. A discernible trend emerges from these curves, indicating a subtle decline in the strain of BZ6 ceramics as the fatigue process unfolds. Figure 3b succinctly illustrates the correlation between the strain values of BZ6 ceramics and the cycle count. Remarkably, after enduring 10^7 unipolar cycles, the strain variation of BZ6 ceramics remains confined within an 8% deviation from its initial value, this is similar to the amount of strain change for CZ5 and BNT.[32] This performance is notably superior to the commercial PIC151 ceramic, which exhibits a strain reduction of approximately 15% under similar fatigue conditions. The data suggest that the BZ6 ceramics exhibit a robust field-induced strain behaviour, demonstrating resilience against the effects of unipolar fatigue. It is noteworthy to highlight that the anti-unipolar fatigue characteristic of BZ6 ceramics is not only commendable in itself but also stands out as superior when compared to other (K, Na)NbO_3-based lead-free piezoelectric materials.[27,33] This comparative analysis not only underscores the exceptional fatigue resistance of BZ6 ceramics but also opens avenues for further exploration and enhancement of piezoelectric materials, paving the way for more durable and reliable applications in various fields.[30,34]

To delve deeper into the exceptional resistance to unipolar fatigue exhibited by the field-induced strain of BZ6 ceramics, a comprehensive study was conducted on the evolution of the large-signal hysteresis return $P(E)$ and strain-electric field $S(E)$ curves as well as the small-signal piezoelectric constant-electric field $d_{33}(E)$ and the dielectric constant-electric field $\varepsilon_{33}(E)$ curves, both before and after the unipolar fatigue. The findings are captured in Figure 4.

Upon close examination of this figure, it is evident that the cycling under unipolar electric fields causes the hysteresis return $P(E)$ to shift along the negative direction of X-axis, as depicted in Figure 4a. And a discernible trend is observed in the piezoelectric constant-electric field $d_{33}(E)$ curve, which progressively shifts along the positive Y-axis with an increase in the cycle number, as shown in Figure 4b. Concurrently, the strain-electric field $S(E)$ curve and the dielectric constant-electric field $\varepsilon_{33}(E)$ curve exhibit a notable asymmetry from left to right, as illustrated in Figure 4c and 4d, respectively. In

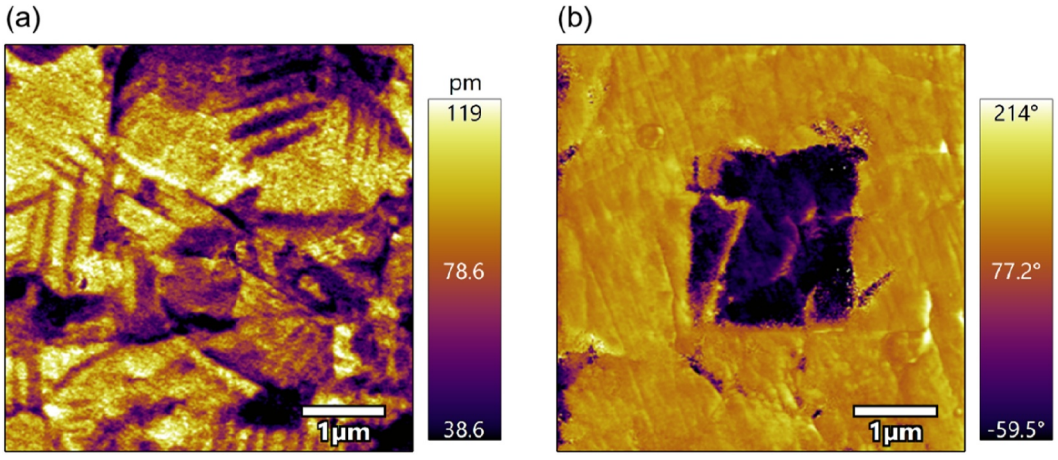

FIGURE 2 (a) Out-of-plane amplitude images and (b) domain morphology image for BZ6.

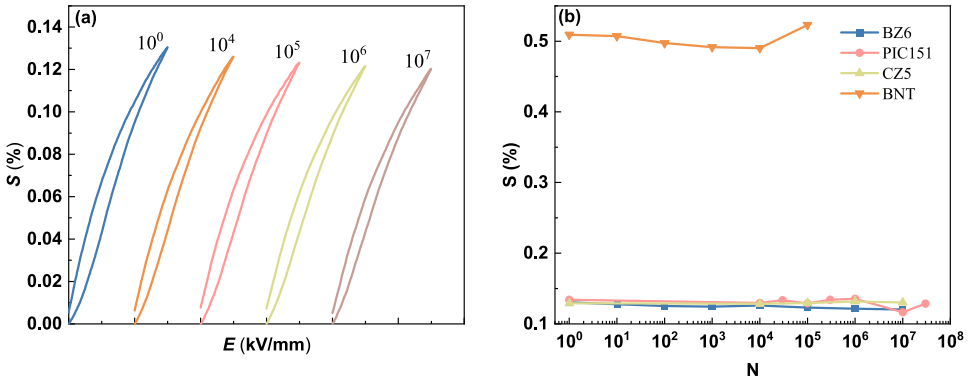

FIGURE 3 (a) Field-induced strain curves of BZ6 ceramics before fatigue and after 10^4, 10^5, 10^6, and 10^7 unipolar electric field cycles, (b) strain and cycle number N of BZ6 ceramics and comparison with soft PZT (PIC151),CZ5, BNT data.

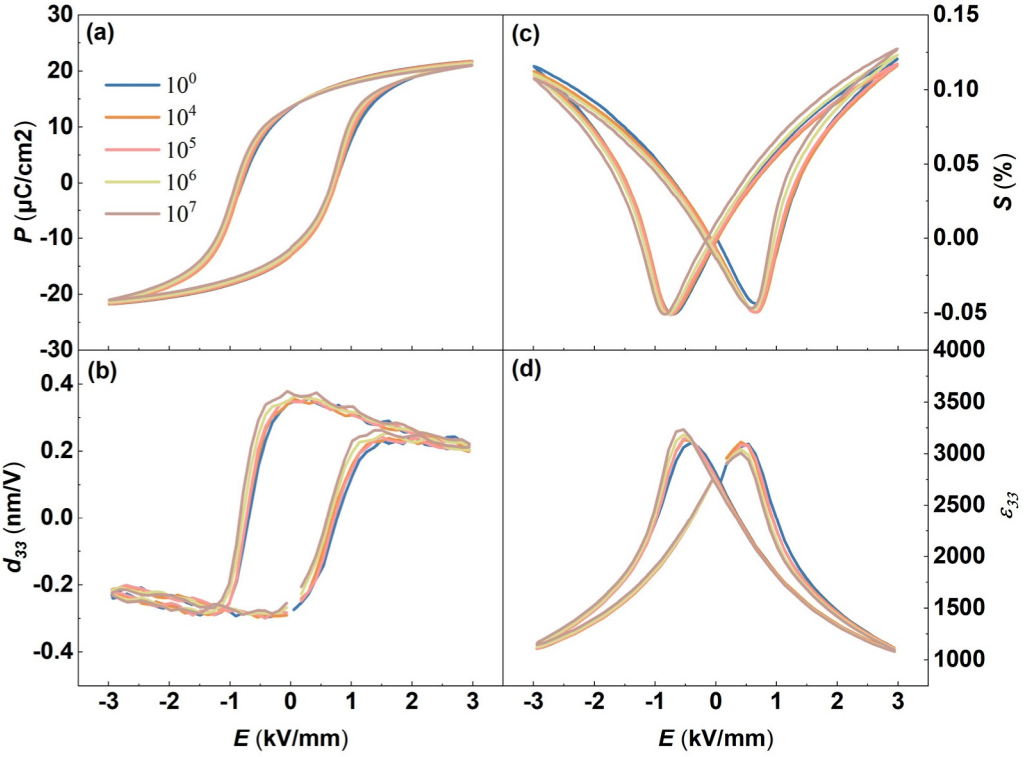

FIGURE 4 (a) Hysteresis return $P(E)$, (b) piezoelectric constant-electric field $d_{33}(E)$ curve, (c) strain-electric field $S(E)$ curve, and (d) dielectric constant-electric field $\varepsilon_{33}(E)$ curve of BZ6 ceramics prior to fatigue and after cycling through the unipolar electric field of 10^4, 10^5, 10^6, and 10^7.

an effort to quantitatively analyse the degree of fatigue endured by the material, a portfolio of key parameters has been extracted from the data presented in Figure 4. These parameters, which serve as canonical indicators of material fatigue, are summarised in Figure 5, which not only sheds light on the underlying mechanisms that endow the BZ6 ceramics with their remarkable fatigue resistance but also provides a robust framework for further investigation and optimisation of piezoelectric materials, ensuring their enduring performance and reliability in various applications.

The degree of asymmetry of the strain-electric field $S(E)$ curve and the dielectric constant-electric field $\varepsilon_{33}(E)$ curve can be quantified by the asymmetry factors γ_s and $\gamma_{\varepsilon 33}$, respectively, which are defined in the following two equations:

$$\gamma_s = \frac{\Delta S^+ - \Delta S^-}{\Delta S^+ + \Delta S^-} \tag{1-1}$$

$$\gamma_{\varepsilon_{33}} = \frac{\Delta \varepsilon_{33}^+ - \Delta \varepsilon_{33}^-}{\Delta \varepsilon_{33}^+ + \Delta \varepsilon_{33}^-} \tag{1-2}$$

where ΔS_{33}^+ and ΔS_{33}^- are the strain changes in the positive and negative electric field directions of the $S(E)$ curve, respectively; and $\Delta \varepsilon_{33}^+$ and $\Delta \varepsilon_{33}^-$ are the changes in the dielectric constant in the positive and negative electric field directions of the $\varepsilon_{33}(E)$ curve, respectively. The graphical representation in Figure 5a delineates the progression of asymmetry factors, denoted as γ_s and $\gamma_{\varepsilon 33}$, for the BZ6 ceramics in relation to the number of unipolar cycles. The corresponding data for the PIC151 ceramics are also included to provide a comparative analysis.[35] A visual inspection of the figure reveals that throughout the range of cycles examined, the asymmetry observed in the $S(E)$ curve of the BZ6 ceramics is consistently less pronounced than that of the PIC151 ceramics. Furthermore, the asymmetry in the $\varepsilon_{33}(E)$ curve for the BZ6 ceramics is significantly more subdued compared to the PIC151, underscoring the superior fatigue resistance of BZ6. In a holistic assessment, the BZ6 ceramics demonstrate a commendable resilience to unipolar fatigue, which is on par with, if not surpassing, that of the PIC151 ceramics. This comparative evaluation not only accentuates the robustness of the BZ6 ceramics against fatigue-induced asymmetries but also highlights their potential as a superior alternative in applications where endurance under cyclic electric fields is critical.

Figures 5b,c present an intricate interplay between the switchable polarisation strength $2P_r$, the negative strain S_{neg}, the internal bias electric field E_{bias}, and the piezoelectric constant d_{33} as they evolve with the number of cycles for the BZ6 piezoelectric ceramics. These data encapsulate a wealth of information, revealing a dynamic and complex relationship where the softening effect and the fatigue effect are in a state of equilibrium during the unipolar fatigue of BZ6 ceramics. The figure illustrates that there is a competitive relationship between the softening effect and fatigue effect in the unipolar fatigue process of BZ6 ceramics. Fatigue studies of PZT piezoelectric ceramics show that unipolar fatigue can lead to the formation of an internal bias electric field E_{bias}, where E_{bias}, can be obtained from the hysteresis return $P(E)$ or the

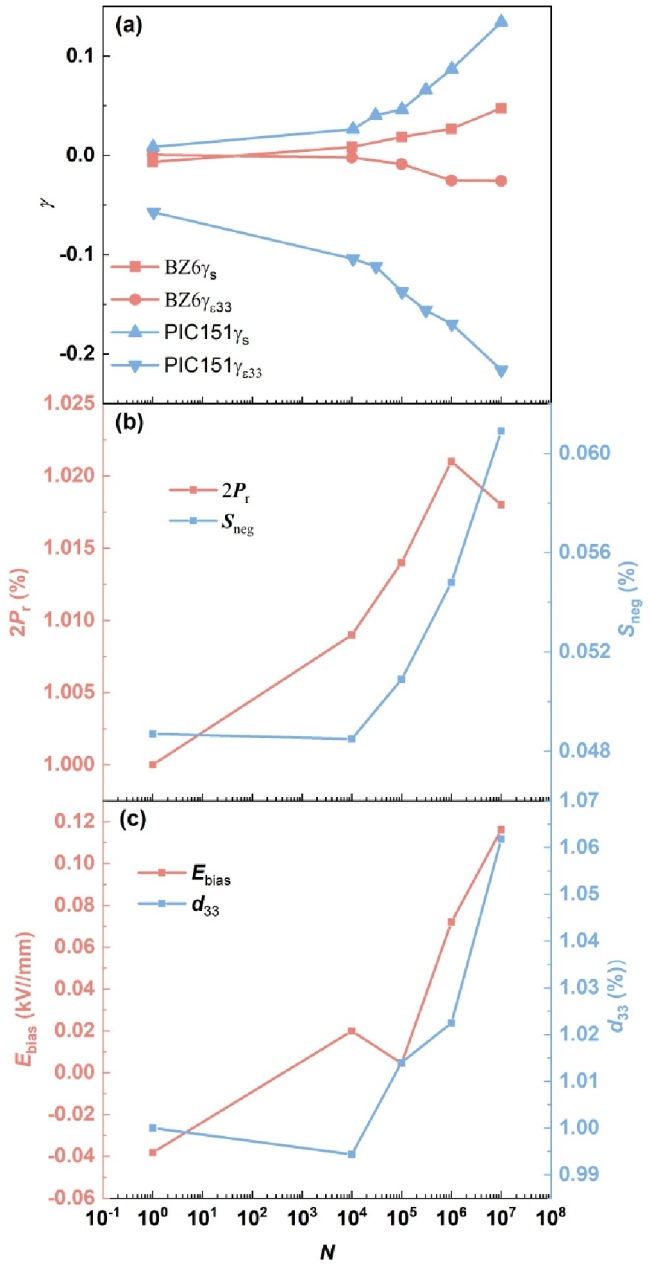

FIGURE 5 (a) Relationship between asymmetry factors γ_s and $\gamma_{\varepsilon 33}$ and the number of unipolar cycles N, (b) reversible polarisation strength $2P_r$, negative strain S_{neg}, (c) internal bias electric field E_{bias}, piezoelectric constant d_{33} versus number of cycles N.

piezoelectric constant—electric field $d_{33}(E)$ curve. However, since the hysteresis return $P(E)$ is measured by a relatively comparative method, the E_{bias} calculated from the $d_{33}(E)$ curve is more reliable, which is defined as follows:

$$E_{bias} = -\frac{E_{C+} + E_{C-}}{2} \quad (1\text{-}3)$$

where E_{C+} and E_{C-} represent the positive and negative coercive fields, respectively, in the $d_{33}(E)$ curve. A careful examination of the figure reveals that the reversible polarisation strength $2P_r$ and the piezoelectric constant d_{33} exhibits a progressive increase within the initial 10^6 cycles. This observation suggests the presence of a softening effect, predominantly attributed to the increased mobility of domain walls. It is noteworthy that this softening effect closely mirrors the outcomes observed during the polarisation process to a significant degree. Upon surpassing the 10^6 cycle threshold, the fatigue effect emerges as a dominant factor, culminating in a diminution of electrical properties, exemplified by a decrease in the $2P_r$ parameter. Concurrently, there is a marked escalation in the internal bias electric field E_{bias}. However, the scenario for the negative strain S_{neg} (defined as the difference between the residual strain and the minimum strain within the strain-electric field $S(E)$ curve) presents a more intricate picture. Generally, the escalation of S_{neg} is typically ascribed to a softening effect, which is associated with the heightened mobility of domain walls. Nevertheless, in the context of the current experiments, the asymmetry observed in the $S(E)$ curve also plays a pivotal role in the observed increase in S_{neg}. This multifaceted interplay between softening and fatigue effects, along with the influence of domain wall dynamics and curve asymmetry, provides a comprehensive understanding of the material's response to cyclic loading, offering valuable insights for the optimisation and application of piezoelectric ceramics.

3.2 | Agglomeration of space charge carriers at grain boundaries

Given the striking similarities in the unipolar fatigue characteristics of BZ6 and PIC151 ceramics, it is plausible to surmise that the mechanisms underlying the performance degradation in both materials may share commonalities. In the realm of PZT piezoelectric materials, the unipolar fatigue phenomenon is predominantly ascribed to the accumulation of space charge. This conceptual framework can be extrapolated to elucidate the unipolar fatigue behaviour of BZ6 ceramics, as depicted in Figure 6. Throughout the process of electric field cycling, the polarisation direction within each domain undergoes incessant transformation. However, due to the disparities in crystal orientation, the polarisation vectors across adjacent grains at the grain boundaries cannot fully compensate each other. This mismatch results in the emergence of a localised depolarisation field, denoted as σ^+ and σ^- (as illustrated in Figure 6a). In response, nearby free charge carriers are mobilised and redistributed to counteract the effects of the depolarisation field, as shown in Figure 6b. The convergence of these charge carriers culminates in the formation of an internal bias field E_{bias}, which aligns with the direction of the applied electric field. The cumulative effect of these bias fields results in a discernible shift in the hysteresis return $P(E)$. This shift can be interpreted as a driving force behind the variability observed in the properties of the BZ6 ceramics, including the asymmetry in the $S(E)$ and $\varepsilon_{33}(E)$ curves. This mechanistic understanding of the unipolar fatigue process not only enriches our comprehension of the degradation dynamics in BZ6 ceramics but also offers a valuable reference for the design and optimisation of robust

piezoelectric materials capable of withstanding the rigours of cyclic electric field applications.

3.3 | Effect of annealing treatment on unipolar fatigue samples

In addition to the agglomeration of space charge can lead to the fatigue effect of piezoelectric ceramics, the mechanical damage during the electric field cycling process should not be ignored. It has been shown that simple annealing treatment can fully or partially restore the piezoelectric properties of PZT ceramics after bipolar[36] and unipolar[22] fatigue if there is no mechanical damage inside the ceramics, such as microcracks or electrode peeling. Therefore, we investigated the effect of annealing treatment on the piezoelectric properties of BZ6 ceramics after fatigue.

Figure 7 presents a comparative analysis of the field strain curves and large-signal electrical curves of BZ6 ceramics in their pristine state, post-fatigue, and subsequent to annealing treatment. The data reveals that the annealing process facilitates a comprehensive restoration of the BZ6 ceramics' properties following fatigue. This observation suggests that the unipolar fatigue process does not result in any mechanical damage to the material, such as microcracks or electrode delamination, which are typically irreparable through thermal treatments. The annealing treatment's ability to fully rejuvenate the material's characteristics underscores the predominance of reversible, non-mechanical alterations, such as the reorientation of polarisation vectors and the redistribution of space charges, during the

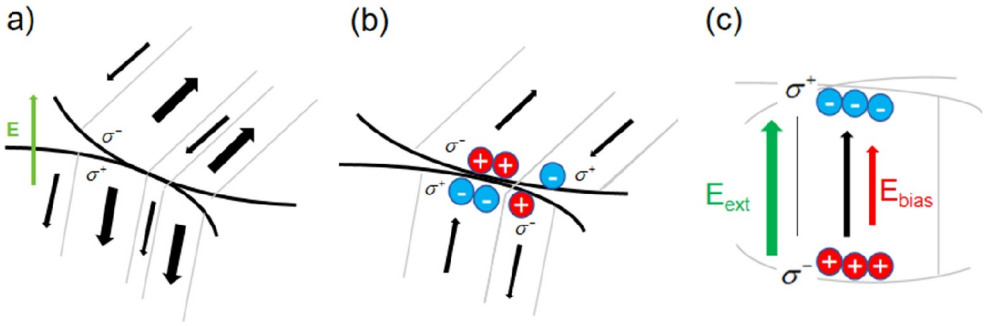

FIGURE 6 Schematic modelling of the agglomeration of space charge carriers at grain boundaries during unipolar fatigue processes. (a) Formation of a localised depolarisation field, (b) redistribution of space charge carriers, (c) formation of an internally biased electric field.

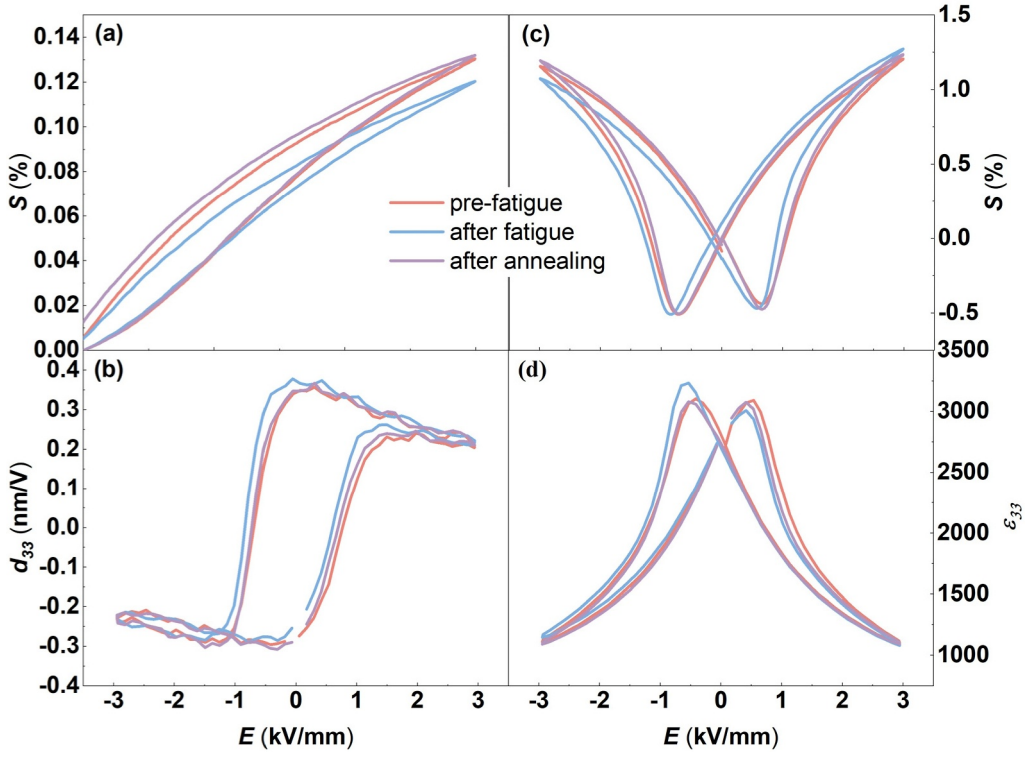

FIGURE 7 (a) Comparison of unipolar field-induced strain curves, (b) piezoelectric constant-electric field $d_{33}(E)$ curves, (c) strain-electric field $S(E)$ curves, and (d) dielectric constant-electric field $\varepsilon_{33}(E)$ curves of BZ6 ceramics before and after fatigue and annealing treatment.

fatigue process. The recovery of the field strain and electrical response to their pre-fatigue states is a testament to the resilience and recoverability of the BZ6 ceramics, highlighting their potential for applications where cyclic loading is involved.

4 | CONCLUSIONS

In conclusion, the present study delves into the unipolar fatigue characteristics of lead-free piezoelectric ceramics, focusing on $BaZrO_3$-modified (K, Na)NbO_3. An impressive resilience is showcased by the $BaZrO_3$-modified (K, Na)NbO_3-based lead-free piezoelectric ceramics. Even after enduring 10^7 cycles of unipolar electric field cycling, the field-induced strain experiences a minimal reduction of approximately 8% relative to its pre-fatigued state. The exposure to unipolar electric field cycling instigates the manifestation of unipolar fatigue attributes in (K, Na)NbO_3-based ceramics, characterised by the formation of internal biased electric fields and the perturbation or asymmetry in the electrical performance hysteresis loops. The observed unipolar fatigue behaviour is elucidated by the agglomeration of space charge carriers at the grain boundaries, which is pivotal in understanding the underlying mechanisms. Remarkably, the electrical properties of the fatigued samples can be entirely revitalised through a straightforward annealing process, a testament to the absence of mechanical damage within the samples. This outcome underscores the ceramics' exceptional endurance against unipolar fatigue and hints at a dynamic interplay between the softening effect and the fatigue effect throughout the unipolar fatigue process. The findings of this study offer profound implications for the development and fabrication of lead-free piezoelectric ceramic materials, particularly for their practical implementation in actuators.

AUTHOR CONTRIBUTIONS

Jun Ma: Data curation; writing - original draft; methodology; software. **Tao Lin**: Writing - review and editing. **Chuanyang Tao**: Writing - review and editing. **Yuqing Zhou**: Writing - review and editing. **Meipeng Zhong**: Writing - review and editing. **Yi-Xuan Liu**: Writing - review and editing. **Zhongshang Dou**: Writing - review and editing. **Binjie Chen**: Writing - review and editing. **Shulin Tan**: Writing - review and editing. **Xin Ma**: Writing - review and editing. **Qiang He**: Writing - review and editing. **Wen Gong**: Writing - review and editing. **Fang-Zhou Yao**: Writing - review and editing. **Ke Wang**: Writing - review and editing.

ACKNOWLEDGEMENTS

This work is supported by National Nature Science Foundation of China (No. 52032005, 52325204, U22A20254), Key R&D Programme of Zhejiang (No. 2022C01229), and the Programme for Jiaxing Leading Innovative and Entrepreneurial Teams.

CONFLICT OF INTEREST STATEMENT

The authors declare no conflicts of interest.

DATA AVAILABILITY STATEMENT

Research data are not shared.

ORCID

Fang-Zhou Yao https://orcid.org/0000-0003-1975-7452

REFERENCES

1. Wang, X., N. Zheng, F. Wei, Y. Zhou, and H. Yang. 2023. "Stability Compensation Design and Analysis of a Piezoelectric Ceramic Driver with an Emitter Follower Stage." *Micromachines* 14(5): 914. https://doi.org/10.3390/mi14050914.
2. Meng, X., and S. Lin. 2019. "Analysis of a Cascaded Piezoelectric Ultrasonic Transducer with Three Sets of Piezoelectric Ceramic Stacks." *Sensors* 19(3): 580. https://doi.org/10.3390/s19030580.
3. Chen, F., C. Yang, Z. An, X. Zhang, T. Zhou, N. Chen, and Design. 2022. "Direct-ink-writing of Multistage-Pore Structured Energy Collector with Ultrahigh Ceramic Content and Toughness." *Materials and Design* 217: 110652. https://doi.org/10.1016/j.matdes.2022.110652.
4. Wang, W., Z. Pang, L. Peng, F. Hu, and Fabrics. 2020. "Non-intrusive Vital Sign Monitoring Using an Intelligent Pillow Based on a Piezoelectric Ceramic Sensor." *Journal of Engineered Fibers and Fabrics* 15: 1558925020977268. https://doi.org/10.1177/1558925020977268.
5. Haoran, L., H. Yan, L. Laibo, and X. J. A. O. A. Dongyu. 2022. "Acoustic Matching Characteristics of Annular Piezoelectric Ultrasonic Sensor." *Archives of Acoustics* 47(2): 275–84. https://doi.org/10.24425/aoa.2022.141656.
6. Yin, J., S. Chen, V.-K. Wong, K. Yao, and Ferroelectrics, and F. Control. 2022. "Thermal Sprayed Lead-free Piezoelectric Ceramic Coatings for Ultrasonic Structural Health Monitoring." *IEEE Transactions on Ultrasonics, Ferroelectrics, and Frequency Control* 69(11): 3070–80. https://doi.org/10.1109/tuffc.2022.3176488.
7. Ou-Yang, J., B. Zhu, Y. Zhang, S. Chen, X. Yang, and W. Wei. 2015. "New KNN-Based Lead-free Piezoelectric Ceramic for High-Frequency Ultrasound Transducer Applications." *Applied Physics* 118(4): 1177–81. https://doi.org/10.1007/S00339-015-9004-8.
8. Zhang, Y., and J.-F. Li. 2019. "Review of Chemical Modification on Potassium Sodium Niobate Lead-free Piezoelectrics." *Journal of Materials Chemistry C* 7(15): 4284–303. https://doi.org/10.1039/C9TC00476A.
9. Li, C., L. Wang, L. Xu, X. Ren, F. Yao, J. Lu, D. Wang, et al. 2024. "Mn-inlaid Antiphase Boundaries in Perovskite Structure." *Nature Communications* 15(1): 6735. https://doi.org/10.1038/s41467-024-51024-2.
10. Zhao, T., K. Shi, C. Fei, X. Sun, Y. Quan, W. Liu, J. Zhang, and X. Dai. 2023. "Structure, Electrical Properties, and Thermal Stability of the Mn/Nb Co-doped Aurivillius-type $Na_{0.5}Bi_{4.5}Ti_4O_{15}$ High Temperature Piezoelectric Ceramics." *Crystals* 13(3): 433. https://doi.org/10.3390/cryst13030433.
11. Li, S., M. Ma, Y. Tian, R. Li, X. Hu, and P. J. J. O. C. P. R. Liu. 2023. "Regulation of $BaTiO_3$ Ceramics' Electrical Properties by Varying $Na_{0.5}Bi_{0.5}TiO_3$ Dopants." *Journal of Ceramic Processing Research* 24(4): 693–9. https://doi.org/10.36410/jcpr.2023.24.4.693.
12. Wu, B., H. Zheng, Y.-Q. Wu, Z. Huang, H.-C. Thong, H. Tao, J. Ma, et al. 2024. "Origin of Ultrahigh-Performance Barium Titanate-Based Piezoelectrics: Stannum-Induced Intrinsic and Extrinsic Contributions." *Nature Communications* 15(1): 7700. https://doi.org/10.1038/s41467-024-52031-z.
13. Zhang, M.-H., K. Wang, Y.-J. Du, G. Dai, W. Sun, G. Li, D. Hu, et al. 2017. "High and Temperature-Insensitive Piezoelectric Strain in Alkali Niobate Lead-free Perovskite." *Journal of the American Ceramic Society* 139(10): 3889–95. https://doi.org/10.1021/jacs.7b00520.
14. Liu, L., B. Yang, R. Lv, Q. Kou, S. Yang, H. Xie, Y. Sun, et al. 2023. "Enhanced Unipolar Electrical Fatigue Resistance and Related Mechanism in Grain-Oriented Pb $(Mg_{1/3}Nb_{2/3})$ O_3-Pb (Zr, Ti) O_3 Piezoceramics." *Journal of Materials Science and Technology* 145: 40–7. https://doi.org/10.1016/j.jmst.2022.10.030.
15. Koo, B.-K., S.-J. Jeong, D.-H. Lee, D.-J. Shin, M.-S. Kim, I.-S. Kim, P.-W. Han, and C. O. Solids. 2022. "Electrical Cycling of Cu-PMNZT

Multilayer Co-fired Ceramic Actuators." *Journal of Physics and Chemistry of Solids* 170: 110950. https://doi.org/10.1016/j.jpcs.2022.110950.
16. Sowmya, N. S., A. Baby, P. Vishnu, S. Siva, E. Sunny, N. Raghu, and T. Karthik. 2024. "Thermal and Fatigue Endurance Strain Response in Low Temperature Sintered 0.4 PZN-0.6 PZT Ceramics for Actuator Applications." *Materials Letters* 355: 135431. https://doi.org/10.1016/j.matlet.2023.135431.
17. Lupascu, D., and J. Rödel. 2005. "Fatigue in Bulk Lead Zirconate Titanate Actuator Materials." *Advanced Engineering Materials* 7(10): 882–98. https://doi.org/10.1002/adem.200500117.
18. Zeng, F. W., H. Wang, and H.-T. Lin. 2013. "Fatigue and Failure Responses of Lead Zirconate Titanate Multilayer Actuator under Unipolar High-Field Electric Cycling." *Journal of Applied Physics* 114(2). https://doi.org/10.1063/1.4813219.
19. Luo, Z., T. Granzow, J. Glaum, W. Jo, J. Rödel, and M. Hoffman. 2011. "Effect of Ferroelectric Long-range Order on the Unipolar and Bipolar Electric Fatigue in $Bi_{1/2}Na_{1/2}TiO_3$-based Lead-free Piezoceramics." *Journal of the American Ceramic Society* 94(11): 3927–33. https://doi.org/10.1111/j.1551-2916.2011.04605.x.
20. Wang, H., T. A. Cooper, H.-T. Lin, and A. A. Wereszczak. 2010. "Fatigue Responses of Lead Zirconate Titanate Stacks under Semibipolar Electric Cycling with Mechanical Preload." *Journal of Applied Physics* 108(8): 084107. https://doi.org/10.1063/1.3486469.
21. Yu, L., S.-W. Yu, and X.-Q. Feng. 2007. "Effects of Electric Fatigue on the Butterfly Curves of Ferroelectric Ceramics." *Materials Science and Engineering: A* 459(1–2): 273–7. https://doi.org/10.1016/j.msea.2007.01.063.
22. Verdier, C., D. C. Lupascu, and J. Rödel. 2002. "Stability of Defects in Lead–Zirconate–Titanate after Unipolar Fatigue." *Applied Physics Letters* 81(14): 2596–8. https://doi.org/10.1063/1.1510161.
23. Nuffer, J., D. C. Lupascu, and J. Rödel. 2002. "Stability of Pinning Centers in Fatigued Lead–Zirconate–Titanate." *Applied Physics Letters* 80(6): 1049–51. https://doi.org/10.1063/1.1448654.
24. Glaum, J., T. Granzow, L. A. Schmitt, H.-J. Kleebe, and J. Rödel. 2011. "Temperature and Driving Field Dependence of Fatigue Processes in PZT Bulk Ceramics." *Acta Materialia* 59(15): 6083–92. https://doi.org/10.1016/j.actamat.2011.06.017.
25. Wu, L., T. Zheng, and J. Wu. 2024. "Structural Origin of Excellent Fatigue Resistance in KNN-Based Ceramics with Multiphase Coexistence." *Journal of the European Ceramic Society* 44(1): 205–14. https://doi.org/10.1016/j.jeurceramsoc.2023.09.033.
26. Cen, Z., Z. Dong, Z. Xu, F.-Z. Yao, L. Guo, L. Li, and X. Wang. 2021. "Improving Fatigue Properties, Temperature Stability and Piezoelectric Properties of KNN-Based Ceramics via Sintering in Reducing Atmosphere." *Journal of the European Ceramic Society* 41(8): 4462–72. https://doi.org/10.1016/j.jeurceramsoc.2021.03.007.
27. Wang, J., Y.-X. Liu, Z. Dou, B. Chen, M. Ju, W. Gong, C. Wu, F.-Z. Yao, K. Wang, and L. Luo. 2023. "$BaZrO_3$-modified (K, Na) NbO_3-Based Lead-free Piezoceramics: Enhanced Electrical Properties and High Fatigue Resistance." *Ceramics International* 49(21): 34139–46. https://doi.org/10.1016/j.ceramint.2023.08.119.
28. Mahesh, M., P. Pal, V. V. B. Prasad, and A. James. 2020. "Improved Properties and Fatigue Resistant Behaviour of Ba $(Zr_{0.15}Ti_{0.85})$ O_3 Ferroelectric Ceramics." *Current Applied Physics* 20(12): 1373–8. https://doi.org/10.1016/j.cap.2020.08.016.
29. Simons, H., J. Glaum, J. E. Daniels, A. J. Studer, A. Liess, J. Rödel, and M. Hoffman. 2012. "Domain Fragmentation during Cyclic Fatigue in 94% $(Bi_{1/2}Na_{1/2})$ TiO_3-6% $BaTiO_3$." *Journal of Applied Physics* 112(4): 044101. https://doi.org/10.1063/1.4745900.
30. Ehmke, M., J. Glaum, W. Jo, T. Granzow, and J. Rödel. 2011. "Stabilization of the Fatigue-resistant Phase by CuO Addition in $(Bi_{1/2}Na_{1/2})$ TiO_3–$BaTiO_3$." *Journal of the American Ceramic Society* 94(8): 2473–8. https://doi.org/10.1111/j.1551-2916.2010.04379.x.
31. Do, M. T., N. Gauquelin, M. D. Nguyen, J. Wang, J. Verbeeck, F. Blom, G. Koster, E. P. Houwman, and G. Rijnders. 2020. "Interfacial Dielectric Layer as an Origin of Polarization Fatigue in Ferroelectric Capacitors." *Scientific Reports* 10(1): 7310. https://doi.org/10.1038/s41598-020-64451-0.
32. Lai, L., Z. Zhao, S. Tian, B. Ou, G. Liang, B. Li, and Y. Dai. 2023. "Ultrahigh Electrostrain with Excellent Fatigue Resistance in Textured Nb^{5+}-doped $(Bi_{0.5}Na_{0.5})$ TiO_3-Based Piezoceramics." *Journal of Advanced Ceramics* 12(3): 487–97. https://doi.org/10.26599/JAC.2023.9220698.
33. Zhang, M.-H., K. Wang, J.-S. Zhou, J.-J. Zhou, X. Chu, X. Lv, J. Wu, and J.-F. Li. 2017. "Thermally Stable Piezoelectric Properties of (K, Na) NbO_3-Based Lead-free Perovskite with Rhombohedral-Tetragonal Coexisting Phase." *Acta Materialia* 122: 344–51. https://doi.org/10.1016/j.actamat.2016.10.011.
34. Luo, Z., J. Glaum, T. Granzow, W. Jo, R. Dittmer, M. Hoffman, and J. Rödel. 2011. "Bipolar and Unipolar Fatigue of Ferroelectric BNT-based Lead-free Piezoceramics." *Journal of the American Ceramic Society* 94(2): 529–35. https://doi.org/10.1111/j.1551-2916.2010.04101.x.
35. Yao, F.-Z., J. Glaum, K. Wang, W. Jo, J. Rödel, and J.-F. Li. 2013. "Fatigue-free Unipolar Strain Behavior in $CaZrO_3$ and MnO_2 Co-modified (K, Na) NbO_3-Based Lead-free Piezoceramics." *Applied Physics Letters* 103(19). https://doi.org/10.1063/1.4829150.
36. Jiang, Q., W. Cao, and L. E. Cross. 1994. "Electric Fatigue in Lead Zirconate Titanate Ceramics." *Journal of the American Ceramic Society* 77(1): 211–5. https://doi.org/10.1111/j.1151-2916.1994.tb06979.x.